



1 **Observation-based implementation of ecophysiological processes for a rubber plant**
2 **functional type in the community land model (CLM4.5-rubber_v1)**

3

4 Ashehad A. Ali¹, Yuanchao Fan², Marife D. Corre³, Martyna M. Kotowska⁴, E. Hassler³,
5 Fernando E. Moyano¹, Christian Stiegler¹, Alexander Röhl⁵, Ana Mejjide⁶, Andre Ringeler¹,
6 Christoph Leuschner⁴, Tania June⁷, Suria Tarigan⁸, Holger Kreft⁹, Dirk Hölscher⁵, Chonggang
7 Xu¹⁰, Charles D. Koven¹¹, Rosie Fisher¹², Edzo Veldkamp³, Alexander Knohl¹

8

- 9 1. University of Göttingen, Bioclimatology, Göttingen, Germany
10 2. Uni Research Climate, Bjerknes Centre for Climate Research, Bergen, Norway
11 3. University of Göttingen, Soil Science of Tropical and Subtropical Ecosystems,
12 Göttingen, Germany
13 4. University of Göttingen, Department of Plant Ecology and Ecosystems Research,
14 Göttingen, Germany
15 5. University of Göttingen, Tropical Silviculture and Forest Ecology, Göttingen, Germany
16 6. University of Göttingen, Department of Crop Sciences, Division Agronomy, Göttingen,
17 Germany
18 7. Department of Geophysics and Meteorology, Bogor Agricultural University, Bogor,
19 Indonesia
20 8. Department of Soil and Natural Resources Management, Bogor Agricultural University,
21 Bogor, Indonesia
22 9. University of Göttingen, Biodiversity, Macroecology & Biogeography, Göttingen,
23 Germany
24 10. Earth & Environmental Sciences Division, Los Alamos National Laboratory, Los
25 Alamos, NM, USA



26 11. Climate and Ecosystem Sciences Division, Lawrence Berkeley National Laboratory,
27 Berkeley, CA, USA

28 12. Climate and Global Dynamics Laboratory, National Center for Atmospheric Research,
29 Boulder, CO, USA

30

31 **Running head:** Rubber plant functional type in the community land model_v4.5

32

33

34 **Abstract**

35 Land-use change has a strong impact on carbon, energy and water fluxes and its effect is
36 particularly pronounced in tropical regions. Uncertainties exist in the prediction of future land-
37 use change impacts on these fluxes by land surface models due to scarcity of suitable measured
38 data for parametrization and poor representation of key biogeochemical processes associated
39 with tropical vegetation types. Rubber plantations (*Hevea brasiliensis*) are a crucial land-use
40 type across tropical landscapes that has greatly expanded in recent decades. Here, we first
41 synthesize the relevant data for describing the biogeochemical processes of rubber from our past
42 measurement campaigns in Jambi province, Indonesia. We then use these data-sets to develop a
43 rubber plant functional type (PFT) for the Community Land Model (CLM4.5). Field measured
44 data from small-holder plantations on leaf litterfall, soil respiration, latex harvest, leaf area index,
45 transpiration, net primary productivity, and above-ground and fine root biomass were used to
46 develop and calibrate a new PFT-based model (CLM4.5-rubber).

47 CLM-rubber predictions adequately captured the annual net primary productivity and
48 above-ground biomass as well as the seasonal dynamics of leaf litterfall, soil respiration, soil
49 moisture and leaf area index. All of the predicted water fluxes of CLM-rubber were very similar
50 to a site-specific calibrated soil water model. Including temporal variations in leaf life span
51 enabled CLM-rubber to better capture the seasonality of leaf litterfall.

52 Increased sensitivity of stomata to soil water stress and the enhancement of growth and
53 maintenance respiration of fine roots in response to soil nutrient limitation enabled CLM-rubber
54 to capture the magnitude of transpiration and leaf area index. Since CLM-rubber predicted
55 reasonably well the carbon and water use, we think that the current model can be used for larger-
56 scale simulations within Jambi province because more than 99% of the rubber plantations are
57 smallholder owned in Jambi province and have low soil fertility.

58

59 **Keywords:** plant functional traits, leaf age, productivity, water use, stomatal conductance

60



61 Introduction

62 Historical records show that Indonesia has had accelerated rates of land-use change from
63 forest to croplands due to economic development and policy reforms (Gellert, 2005). Within
64 Indonesia, Jambi province on Sumatra has been a hotspot of land-use change with a relatively
65 large area of forest converted to rubber plantations over the past two decades (Melati, 2017), in
66 part due to projected increases in the demand of this commodity (Eleanor et al., 2015). Little is
67 known about how these land-use changes alter the biogeochemical processes of the carbon and
68 water cycles (Mann, 2009; Powers et al., 2011; Qui, 2009), which are fundamental for ecosystem
69 services. Previous studies have shown that land-use changes to rubber plantation decrease above
70 and below-ground carbon pools (de Blécourt et al., 2013; Ziegler et al., 2009) and affect the soil
71 nitrogen cycle (Allen et al., 2015; Corre et al., 2006). Thus, quantifying land-atmosphere
72 interactions of rubber plantations in the context of ongoing land-use and climate change is
73 essential for understanding local, regional and even global carbon and water balances.

74 So far, insufficient field data are the main limiting factor of our current understanding of
75 carbon and water cycling in rubber plantations (Blagodatsky et al., 2016; Carr, 2012). Although
76 traditional field-based methods are critical for identifying how biogeochemical processes are
77 affected by land-use changes to rubber plantations (e.g. Allen et al., 2015), they also have
78 limitations, especially when analyzing interactions between different processes and extrapolating
79 values to long-term temporal and large spatial scales. In contrast, remote sensing approaches
80 provide essential information on past land-use changes and surface properties of rubber
81 plantations (Ranganath et al., 2004; Senf et al., 2013), but they do not completely describe
82 ecosystem-scale changes, nor the mechanisms behind the changes. Quantitative understanding of
83 the physiological processes leading to biogeochemical disruption is critical for making future
84 projections of the environmental implications associated with different land-use change
85 scenarios, and that is only possible with modelling techniques such as process-based land surface
86 models used in conjunction with the data sources described.

87 Numerous land surface models differ in their prediction of land-use change effects on
88 carbon (Houghton et al., 2012) and water cycles (Boisier et al., 2012; Pitman et al., 2009). Such
89 uncertainties in land surface models may stem from errors in measurements of meteorological
90 variables (Rahul et al., 2014), incorrect initial conditions (Hanna et al., 2017), poor
91 representation of processes (Ali et al., 2016) or errors in parameters (Bonan and Doney, 2018).



92 Errors in model parameters are considered to be the largest uncertainty in various land surface
93 models (Bonan and Doney, 2018), including the Community Land Model (CLM). The CLM
94 version 4.5, used here, represents naturally- and crop-vegetated land units (Oleson et al., 2013)
95 as patches of plant functional types (PFTs) defined by key ecological functions (Bonan et al.,
96 2002). The existing parameterization of CLM allows an adequate description of the specific
97 land-use change effects on annual and perennial crops (Oleson et al., 2013). However, the
98 biogeochemical cycles of most of the woody tree crops, including rubber are not yet
99 implemented in CLM (but see Fan et al., 2015).

100 Rubber (*Hevea brasiliensis*) is a commercially important tree species native to the
101 Amazon rainforest (Wycherley, 1992) but cultivated throughout the tropics. The species is
102 evergreen in its native range, but drought deciduous in other tropical regions, including
103 Indonesia (Kotowska et al., 2016), Thailand (Giambelluca et al., 2016) and China (Lin et al.,
104 2018). The mechanistic basis for the leaf habit of rubber remains poorly understood. In regions
105 having a marked dry season, the period of defoliation is short and re-foliation occurs before the
106 commencement of the rainy season, triggered by an increase in day length (Maite et al., 2008). In
107 contrast, if the dry season is less pronounced, leaf fall occurs more gradually, new leaves develop
108 more slowly and, although the trees are never completely leafless, latex yields are reduced more
109 than in situations where complete defoliation occurs.

110 In this study, we develop a sub-model called “CLM4.5-rubber_v1”, within the framework
111 of CLM4.5, which simulates the productivity, growth, yield, and water and energy cycles of
112 rubber. To reflect the specific growth characteristic of rubber trees, we modify and develop the
113 parameters and processes of the existing tropical deciduous forest PFT. The existing drought-
114 deciduous phenology scheme of the tropical PFT is modified together with the carbon and
115 nitrogen allocation module, where carbon exports through latex harvest influence both carbon
116 and nitrogen allocation.

117 The main objectives of this paper are to (1) implement phenology, carbon and nitrogen
118 allocation, and yield dynamics for to represent the physiology of rubber plants in CLM-rubber,
119 (2) use the developed model to test the hypothesis that drought will reduce the latex yield of
120 rubber plantation, and (3) use CLM-rubber to generate hypotheses that field experimentalists can
121 investigate in the future. To achieve these objectives, we synthesized the data collected both by
122 short-term field campaigns and intensive one-year measurements in small-holder rubber



123 plantations, which are commonly unfertilized, in Jambi, Indonesia and used part of the data for
124 calibration and the rest for validation of CLM-rubber.

125

126 **Methodology**

127 *Overview*

128 We made several modifications to the parametrization of the drought deciduous tropical
129 PFT and implemented phenology, carbon & nitrogen allocations and latex yield processes as we
130 developed the rubber PFT in CLM using the measured data. We made these changes in a
131 systematic way as described below and show the results that includes the effect of the overall
132 change. To save space, we include figures for the model calibration in the main manuscript and
133 put figures for the model validation in the supplementary section.

134

135 *Study Sites*

136 Our study site is located on mineral soils (Acrisols) located in the lowlands of Jambi
137 province, Indonesia (2° 0' 57" S, 103° 15' 33" E, 40 - 100 m above sea level). The studied rubber
138 plantations were owned by smallholders who did not fertilize 2-5 years prior to and during our
139 field measurements that started in 2013. A large part of the Jambi province had been converted
140 to rubber plantations in the past two decades (Margono et al., 2012), and thus this study area was
141 selected as a hotspot of rubber expansion by our ongoing collaborative research center
142 (Ecological and Socio-economic Functions of Tropical Lowland Rainforest Transformation
143 Systems, <http://www.uni-goettingen.de/en/310995.html>). The mean annual temperature in Jambi
144 is 26.7 ± 1.0 °C and the mean annual precipitation is 2235 ± 385 mm (Drescher et al., 2016). The
145 dry season is usually from July to August and the rainy season occurs from October to April.

146 Measurements were performed in two landscapes within the Jambi province that differed
147 mainly in soil texture: loam and clay Acrisol soils (Allen et al., 2015). The loam Acrisol soil was
148 located about 80 km southwest of Jambi City, and hereafter referred to as the Harapan landscape.
149 The clay Acrisol soil was located about 90 km west of Jambi City, and hereafter referred to as
150 the Bukit Duabelas landscape. Within each of the two landscapes, four rubber plantations were
151 chosen and within each plantation a 50 m x 50 m plot was established, totaling eight plots
152 (Kotowska et al., 2015). On average, the rubber plantations in Bukit Duabelas landscape were
153 five years younger than those in Harapan landscape.



154 We collated the following measured data-sets from each of the eight plots: above-ground
155 biomass, net primary productivity, leaf litterfall, latex yield, fine root biomass; soil moisture, soil
156 respiration, leaf area index, and transpiration. All of the data were obtained between 2012 and
157 2014, except leaf area index, which was measured in 2018. Additional information on vegetation
158 characteristics such as rubber tree density, tree height, and basal area can be found in Table 2 of
159 Kotowska et al. (2015).

160

161 *Rubber PFT development*

162 For the development of the rubber plant functional type in CLM, our main goal was to
163 capture the growth characteristics of rubber trees and include a realistic representation of carbon
164 exports via latex harvest. We adapted the rubber PFT to be partly based on the existing broadleaf
165 tropical deciduous tree PFT. We modified the phenology scheme and implemented the harvest
166 export using the field data described above.

167

168 *Phenology, Carbon & Nitrogen Allocation and Yield*

169 First, we considered the default tropical drought deciduous phenology scheme in CLM4.5
170 (Dahlin et al., 2015) that allows plants to shed their leaves through two alternative mechanisms:
171 1) stress-deciduous leaf onset/offset switches triggered by a sustained period of dry soil; 2) a
172 background leaf litterfall rate calculated based on leaf longevity that is not associated with a
173 specific offset period but occurs over an extended period of time. Leaf onset and offset for the
174 drought stress of deciduous phenology type (Dahlin et al., 2015) is based on the critical soil
175 water potential and soil water index accumulator (see Table S1). Preliminary results of the CLM-
176 rubber development showed that the default drought stress onset/offset mechanism did not
177 capture well enough the declining trend of LAI of rubber plantation in the dry season. The
178 determination of leaf shedding for tropical deciduous trees is generally a challenging problem
179 (Dahlin et al., 2017) and very few studies have looked into this aspect to date (Medlyn et al.,
180 2016; Xu et al., 2016). Based on the measurements of leaf litterfall (Kotowska et al., 2016), we
181 incorporated seasonal changes in the leaf life span of rubber in order to improve the background
182 leaf litterfall mechanism, wherein we set a higher leaf life span value in the wet season than in
183 the dry season. A calendar month-dependent function of month was used to model leaf life span
184 (“leaf_long” (yrs)). This function computes leaf_long in a step-wise fashion as follows,



$$185 \quad \text{leaf_long} = \begin{cases} 2, \text{month} < 4 \\ 1.55, 4 \leq \text{month} \leq 5 \\ 0.55, 6 \leq \text{month} \leq 7 \\ 0.23, 8 \leq \text{month} \leq 9 \\ 4.1, \text{month} > 9 \end{cases} \quad (1)$$

186 The above implementation was necessary to ensure that the modeled background leaf litterfall
 187 considers the variability in leaf life span.

188 Four to five times in a week, stems of rubber trees are tapped and the latex is harvested
 189 (yield). Previous experimental work showed that tapped rubber trees grew less than untapped
 190 trees (Chantuma et al., 2009; Silpi et al., 2007). Since latex is rich in carbon, this was interpreted
 191 as active carbon allocation to storage in response to tapping (Chantuma et al., 2009; Silpi et al.,
 192 2007). In our model, latex yield is proportional to annual net primary productivity (Kotowska et
 193 al., 2015) and also considered from the partitioning of growth and storage carbon pools. We
 194 included the latter because in the field, latex yield could also result from the storage pools
 195 (Junjittakarn et al., 2012; Sara et al., 2014).

196 To our knowledge, calculation of latex yield from net primary productivity and
 197 calculation of latex yield from the partitioning of growth and storage carbon pool is a new
 198 concept and has not been considered in any of the rubber modeling studies (Kumagai et al.,
 199 2013). Subsequently, we introduced in the CLM-rubber two tapping-related parameters; tap_npp,
 200 the proportion of latex yield taken from net primary productivity and tap_partition, the
 201 proportion of latex yield taken from the partitioning of the growth and storage carbon pools (see
 202 Table S1).

203 CLM4.5 calculates carbon allocated to new growth based on five allometric parameters
 204 that relate allocation between tissue types (Oleson et al., 2013): 1) ratio of new fine root to new
 205 leaf carbon allocation (a_1), 2) ratio of new coarse root to new stem carbon allocation (a_2), 3) ratio
 206 of new stem to new leaf carbon allocation (a_3), 4) ratio of new live wood to new total wood
 207 allocation (a_4) and 5) ratio of growth respiration carbon to new growth carbon (g_1). CLM4.5 has
 208 a dynamic allocation scheme (Oleson et al., 2013), which includes one dynamic allometric
 209 parameter (a_3 as a function of annual NPP). For the drought deciduous tropical PFT, a_1 , a_2 , a_4 and
 210 g_1 are constants ($a_1 = 1$, $a_2 = 0.3$, $a_4 = 0.1$ and $g_1 = 0.3$), whereas a_3 is a dynamic parameter
 211 defined by the following equation,

$$212 \quad a_3 = \frac{2.7}{1 + e^{-0.004(\text{NPP}_{\text{ann}} - 300)}} - 0.4, \quad (2)$$



213 where NPP_{ann} is the annual sum of NPP of the previous year. The above equation for a_3 increases
 214 stem allocation relative to leaf when annual NPP increases. We assume that due to tapping, the
 215 ratio of new stem to new leaf carbon allocation would change, thus, for CLM-rubber, we
 216 modified a_3 as follows,

$$217 \quad a_3 = \frac{2.7}{1 + e^{-0.004((1 - tap_npp)NPP_{ann} - 300)}} - 0.4, \quad (3)$$

218 where tap_npp is the proportion of latex yield taken from annual net primary productivity.

219 In addition to tapping from NPP, we also considered tapping from the partitioning of
 220 growth and storage carbon pool. We recognized that for all deciduous PFTs, there is a fraction of
 221 allocation that goes into the growth pool (f_{cur}), which is currently set to 0 (unitless) and the
 222 remainder ($1 - f_{cur}$) goes to the storage pool. Subsequently, the deciduous phenology module
 223 either uses the onset growth function or a background growth transfer rate ($bgtr$; outside of onset
 224 period) to move storage carbon to displayed growth pools. For CLM4.5-rubber, we partition f_{cur}
 225 into three portions; growth (f_{cur_gr}), storage (f_{cur_st}) and tapping (f_{cur_tap}). We assume that
 226 the total fraction of allocation that goes into the growth, storage and tapping pool is 1 (unitless).
 227 Next, we define f_{cur_tap} as a parameter called “ $tap_partition$ ” (see Table S1). We also define
 228 the fraction of allocation that goes into the storage as “ f_{cur_st} ” and set $f_{cur_st} = 0.5$. Because
 229 f_{cur_tap} and f_{cur_st} are known, we obtain the fraction of allocation that goes into the growth
 230 pool (f_{cur_gr}) as follows,

$$231 \quad f_{cur_gr} = 1 - (f_{cur_tap} + f_{cur_st}) \quad (4)$$

232 It is important to recognize that in Eq. 4 as f_{cur_tap} increases, f_{cur_gr} decreases. This
 233 trade-off is in line with the notion that tapping limits growth (Chantuma et al., 2009; Silpi et al.,
 234 2007). Given the above allocation parameters (a_1 , a_2 , a_3 , a_4 and g_1) and carbon to nitrogen ratios
 235 of these tissues: leaf, fineroot, livewood (in stem and coarse root) and deadwood (in stem and
 236 coarse root), which are constants, the total carbon and nitrogen allocation to new growth
 237 (CF_{alloc} , $gC\ m^{-2}s^{-1}$, and NF_{alloc} , $gN\ m^{-2}s^{-1}$, respectively) can be expressed as functions of
 238 new leaf carbon allocation ($CF_{GPP,leaf}$, $gC\ m^{-2}s^{-1}$):

$$239 \quad CF_{alloc} = CF_{GPP,leaf}C_{allom}, \quad (5)$$

$$240 \quad NF_{alloc} = CF_{GPP,leaf}N_{allom},$$

241 where C_{allom} , N_{allom} are the carbon and nitrogen allometry (Oleson et al., 2013). From the
 242 stoichiometric relationship in Eq. 5, the associated carbon allocation flux is:



$$243 \quad CF_{\text{alloc}} = NF_{\text{alloc}} \frac{C_{\text{allom}}}{N_{\text{allom}}} \quad (6)$$

244 Total allocation to new leaf carbon ($CF_{\text{alloc,leaf_tot}}$, $gCm^{-2}s^{-1}$) is calculated as:

$$245 \quad CF_{\text{alloc,leaf_tot}} = CF_{\text{alloc}} / C_{\text{allom}} \quad (7)$$

246 In CLM4.5, there are two carbon pools associated with each plant tissue: 1) growth and
 247 2) storage. The carbon pools that represent growth include carbon in leaf (leafc), carbon in fine
 248 roots (frootc), carbon in live stem (livestemc), carbon in dead stem (deadstemc), carbon in live
 249 coarse roots (livecrootc) and carbon in dead coarse roots (deadcrootc). The carbon pools that
 250 represent storage have a suffix “_storage” and include leafc_storage, frootc_storage,
 251 livestemc_storage, deadstemc_storage, livecrootc_storage and deadcrootc_storage. In CLM4.5,
 252 the carbon allocation fluxes have a prefix “cpool_to_”.

253 For CLM-rubber, we made changes to all of the above carbon pools, we show below the
 254 key carbon allocation fluxes for CLM-rubber in the leaf, fineroot and tapping pools. Given
 255 $CF_{\text{alloc,leaf_tot}}$, $f_{\text{cur_gr}}$, $f_{\text{cur_st}}$ and $f_{\text{cur_tap}}$, the allocation fluxes of carbon to growth and
 256 storage pools for the various tissue types can be calculated as follows,

$$257 \quad \text{cpool_to_leafc} = CF_{\text{alloc,leaf_tot}} * f_{\text{cur_gr}}, \quad (8)$$

$$258 \quad \text{cpool_to_leafc_storage} = CF_{\text{alloc,leaf_tot}} * f_{\text{cur_st}},$$

$$259 \quad \text{cpool_to_frootc} = CF_{\text{alloc,leaf_tot}} * a_1 * f_{\text{cur_gr}},$$

$$260 \quad \text{cpool_to_frootc_storage} = CF_{\text{alloc,leaf_tot}} * a_1 * f_{\text{cur_st}}$$

261 The carbon flux of the latex yield is the sum of yield from net primary productivity and
 262 partitioning pool, which is calculated as follows,

$$263 \quad \text{cpool_to_tappingc} = \text{tap_npp} * \text{NPP_ann} * \frac{1}{3600*24*365} + CF_{\text{alloc,leaf_tot}} * f_{\text{cur_tap}} \quad (9)$$

264 Besides the new tapping mechanism, one of the major differences between CLM4.5 for
 265 tropical deciduous PFT and CLM-rubber with respect to the above carbon allocation fluxes is
 266 that CLM4.5 does not have a carbon export flux for latex yield. Further, CLM4.5 used a fixed
 267 “fcur” term in all of the equation 8 to partition carbon fluxes to growth pools and to storage pools
 268 associated with each tissue type. In contrast, CLM-rubber partitions allocation fluxes to the new
 269 tapping pools as well as growth and storage, which are defined above in Eq. 4.

270 The nitrogen pools follow the stoichiometric relationship with carbon pools. The nitrogen
 271 pools for the growth include nitrogen in leaf (leafn), nitrogen in fine roots (frootn), nitrogen in



272 live stem (livestemn), nitrogen in dead stem (deadstemn), nitrogen in live coarse roots
273 (livecrootn) and nitrogen in dead coarse roots (deadcrootn). Similar to the carbon pools, the
274 nitrogen pools also have corresponding storage pools and displayed growth pools The
275 corresponding nitrogen allocation fluxes are calculated as ratios of carbon allocation fluxes using
276 the inverse of respective carbon to nitrogen ratios of different tissue types.

277 In the CLM-rubber, tapping of rubber trees started at the age of six years. The model
278 updates the ratio of carbon to nitrogen of latex yield every half hour.

279

280 *Initial model simulations*

281 To mimic the vegetation and soil state prior to rubber plantation, a Tropical Evergreen
282 forest PFT was first spun-up and run until 1997 using the standard procedures of CLM4.5 spin-
283 ups (Fan et al., 2015; Koven et al., 2013). We used the Tropical Evergreen PFT for the spin-up
284 because we assumed that the natural vegetation prior to land-use change was evergreen. A
285 comparison of the modeled above ground biomass and net primary productivity of the spin-up
286 phase with the observed above ground biomass and net primary productivity of tropical
287 evergreen forests at our site (Kotowska et al., 2015) showed that these matched reasonably well
288 (see Figure S1). Following the spin-up phase, a clear-cut in 1998 was simulated by setting the
289 above ground carbon and nitrogen pools to zero.

290 Second, using the site-level measurements on soil texture (Allen et al., 2015) and climate
291 data for 2013 (Meijide et al., 2018) at the Harapan landscape, a rubber plantation simulation was
292 performed from 1998 to 2014. First, we used the default parametrization of stress deciduous
293 tropical PFT of CLM4.5, but the generic model performance was poor relative to some of the
294 measurements (see below for details). Hence, we performed a model calibration exercise using
295 data collected specifically for rubber plantations.

296

297 *Observational data for model calibration*

298 We briefly outline all of the measured data that we used for parametrization and
299 calibrating the CLM-rubber in the Harapan landscape. Except for fine root biomass, all other
300 data, which consist of carbon pools and net primary productivity in above- and below ground
301 tree biomass at our plots are adapted from Kotowska et al. (2015). We used measurements of
302 fine root biomass from Kurniawan et al. (2018) because it was measured down to a depth of 100



303 cm. This data-set is not from a different site and was measured across all eight rubber plots. The
304 overall measurement campaign for the rubber inventory data spanned from August 2012 to
305 March 2014. Leaf litterfall of data were collected using 16 litter traps (placed in a random grid)
306 at each of the eight plots (see Kotowska et al., 2016 for details). Litter was collected at monthly
307 intervals from March 2013 to April 2014.

308 Soil respiration was measured using vented static chamber, to which four permanent
309 chamber bases were placed randomly at each of the eight plots. Concurrent to soil respiration
310 measurement, soil moisture was measured by the gravimetric method using four samples taken
311 near to the chambers within a depth of 5 cm. Both soil respiration and moisture content were
312 measured monthly at all plots from December 2012 to December 2013 (Hassler et al., 2015).

313 Rubber tree water use ('transpiration') was measured using two commonly applied sap
314 flux techniques, the thermal dissipation probe (TDP) method (Granier, 1985) and the heat field
315 deformation (HFD) method (Nadezhdina et al., 2012). Two TDPs per tree yielded averages of
316 sap flux density in the outer xylem (0-2.5 cm) for each sample tree. The HFD method, with
317 multiple measurement points from 0-8 cm into the xylem, yielded typical radial sap flux profiles
318 for rubber trees and thus allowed the calculation of cross-sectional water conductive areas.
319 Combining the output of the two methods allowed us to calculate water use rates of the six
320 sample trees per plot, which was further extrapolated to stand transpiration (using the tree
321 density and diameter distribution from Kotowska et al., (2015)) (Niu et al., 2017).

322

323 *Model calibration steps & resource limitations*

324 During the initial model – measurement comparison, we noted several discrepancies
325 between the model and measurements. Compared to the modeled values, the measured
326 transpiration and leaf area index were substantially lower while soil respiration was higher. To
327 minimize the mismatch between the model and measurements, we decided to calibrate the
328 model. Due to the long computing time required to run the CLM model (from 1998 to 2014), in
329 this study, we used a simple calibration method (Fan et al., 2015; Rahul et al., 2014) as opposed
330 to more complex methods such as Monte Carlo Markov Chain approaches (Ali et al., 2016).

331 Our initial model calibration step involved obtaining a “realistic” seasonal dynamics of
332 leaf area index. Although we did not have the seasonal data on leaf area index, our educated
333 guess (as well as through “pers. comm.”) indicates that the seasonal dynamics of leaf area index



334 would be relatively “smooth” with a depth of the dip not so large in the dry season, that is, it will
335 have something like a “brevi-deciduous” phenology. We do not expect the leaf area index in the
336 dry season to decrease suddenly with a strong intense as observed in rubber plantations from
337 other sub-tropical regions (see Fig.2; Giambelluca et al., 2016). We increased the critical value
338 of the soil water potential (from -2 MPa to -0.5 MPa) to trigger leaf shedding in the model. In
339 this case, the seasonal dynamics of the modeled leaf area index resulted in a sudden decrease in
340 leaf area index with a narrow depth of the dip – a seasonal trend of leaf area index that we do not
341 expect at our study sites.

342 In CLM4.5, soil water influences stomatal conductance directly by multiplying the
343 minimum conductance by a soil water stress function β_t and also indirectly through net
344 photosynthesis (Oleson et al., 2013). The latter effect is achieved by multiplying the maximum
345 carboxylation rate (V_{cmax}) and dark respiration (R_d) by β_t . The function β_t ranges from one
346 when the soil is wet to near zero when the soil is dry and depends on the soil water potential of
347 each soil layer, the root distribution of the plant functional type, and a plant-dependent response
348 to soil water stress

$$349 \quad \beta_t = \sum_i w_i r_i \quad (10)$$

350 where w_i is a plant wilting factor for layer i and r_i is the fraction of roots in layer i . The plant
351 wilting factor w_i is

$$352 \quad w_i = \begin{cases} \frac{\varphi_c - \varphi_i}{\varphi_c - \varphi_o} \left(\frac{\theta_{sat,i} - \theta_{ice,i}}{\theta_{sat,i}} \right) \leq 1, T_i > T_f - 2 \text{ and } \theta_{liq,i} > 0 \\ 0, T_i \leq T_f - 2 \text{ or } \theta_{liq,i} \leq 0 \end{cases} \quad (11)$$

353 where φ_i is the soil water matric potential (mm) and φ_c and φ_o are the soil water potential (mm)
354 when stomata are fully closed or fully open (respectively). The term in brackets scales w_i by the
355 ratio of the effective porosity (accounting for the ice fraction; $\theta_{sat} - \theta_{ice}$) relative to the total
356 porosity.

357 To induce stomatal closure via soil water in CLM-rubber, we increased the sensitivity of
358 stomata to soil water stress (Verhoef and Egea, 2014) by modifying the default soil water
359 potential for drought deciduous tropical PFT in the model for stomatal opening "smpso = -17500
360 mm" to "smpso = -8750 mm" and stomatal closing "smpsc = -112000 mm" to "smpsc = -56000
361 mm". These changes are equivalent to modifying stomatal opening from -0.34 MPa to -0.17 MPa
362 and full closure from -2.19 MPa to -1.09 MPa. The above two changes are within the range of
363 plausibility, if we consider rubber trees to be sensitive to drought. The values of soil water



364 potential for stomatal opening and full closure in CLM depend on plant functional type. The
365 default values for stomatal opening of PFTs range from -0.35 to -0.83 MPa while for full closure
366 Oleson et al. (2013) quote values ranging between -2.24 and -4.28 MPa. These stomatal opening
367 and full closure values in CLM are known to vary a lot by species and are based on White et al.
368 (2000).

369 Rubber plantations at our sites are known to have low soil nitrogen availability and are
370 not fertilized. In particular, the rubber plantations have low gross nitrogen mineralization rate,
371 microbial nitrogen and mineral nitrogen (Allen et al., 2015; Hassler et al., 2015) and therefore,
372 growth and productivity of our rubber plantations could be limited by nitrogen and possibly by
373 other nutrients e.g. low phosphorus and base saturation (Allen et al., 2016). These were
374 attributed to the fact that our studied plantations were on highly weathered acrisol soils (which
375 have inherently low levels of extractable phosphorus and exchangeable base cations) and were
376 not fertilized for two to five years prior to the start of our field measurements in 2012 (Allen et
377 al., 2015; Hassler et al., 2015; Kurniawan et al., 2018). In an attempt to capture the magnitude of
378 the relatively low leaf area index and low transpiration, we made the following change based on
379 the idea that if nutrients are limiting in the soil, then in real ecosystems roots will have to pay a
380 cost. In this version of the model, we assume that maintenance respiration of fine roots is high to
381 pay for nitrogen uptake, so the base rate of maintenance respiration was increased by 50% for the
382 fine roots in line with Doughty et al. (2018). In CLM4.5, the base rate of maintenance respiration
383 per unit nitrogen content is fixed for all tissues (leaf, livestem, livecroot and fineroot) and is
384 defined as $MR_{\text{base}} = 2.525 \text{ e}^{-6} \text{ gC gN}^{-1} \text{ s}^{-1}$. For CLM-rubber, we set MR_{base} to
385 $3.7875 \text{ e}^{-6} \text{ gC gN}^{-1} \text{ s}^{-1}$ when we calculate the maintenance respiration for fineroots. This
386 change to represent local nutrient limitation made the model predict a relatively high soil
387 respiration rate (sum of autotrophic and heterotrophic respiration), thus reducing net primary
388 productivity and lowering leaf area index.

389 Preliminary calibration results showed that the modeled soil respiration still
390 underestimated the measured soil respiration by approximately 25%. To improve this, we
391 increased the growth respiration of fine roots, which is currently fixed and set as 0.3 for tropical
392 deciduous PFTs in CLM4.5 by a factor of 3 for CLM-rubber. This is a relatively large change.
393 There is one reason to support this increase on growth respiration of fine roots. On average, these
394 rubber plantations lose 20% of the original organic carbon in the soil after 4 years from forest



395 conversion (van Straaten et al., 2015), yet soil respiration was comparable to that of the reference
396 forest (Hassler et al., 2015). These findings suggest that the proportion of heterotrophic
397 respiration would be lower than the contribution of autotrophic respiration to the soil respiration.
398 The decreases in available nitrogen, extractable phosphorus and base saturation (Allen et al.,
399 2016; Allen et al., 2015) suggest that there may be strong competition for phosphorus such that
400 trees have to allocate more carbon for their root growth and root–mycorrhizal system to obtain
401 these nutrients (Fisher et al., 2016; Shi et al., 2016).

402 In the model – measurement comparison for soil organic carbon, CLM-rubber initially
403 predicted only 9% decline in soil carbon for rubber plantation since clear-cut; however, a study
404 by van Straaten et al. (2015), who conducted soil carbon measurements on heavily weathered
405 soils for rubber plantations in Jambi and showed that on average, rubber plantations have 20%
406 lower soil carbon stocks than forests. To increase the modeled decline in soil carbon, we
407 increased the value of Q10 (“the increase of soil respiration per 10°C increase in temperature”)
408 of soil temperature, from 1.5 to 3, on the grounds that rubber plantations at our study sites are
409 0.5°C hotter than forests (Meijide et al., 2018).

410

411 *Model validation in the Bukit Duabelas landscape*

412 Using the soil texture measurements from the Bukit Duabelas landscape (Allen et al.,
413 2015), a model spin-up was performed till year 2002. The spin-up for the model validation was
414 carried out in the same way as the spin-up for the model calibration. Then a clear-cut was
415 introduced in 2003. Using climate data from 2013 (Meijide et al., 2018), we performed a
416 simulation from year 2003 till 2014 by recycling the climate data every year. We used the same
417 rubber PFT parameterization as obtained for the Harapan landscape except the tap_npp
418 parameter. The latter was adjusted because (1) the proportion of measured latex yield relative to
419 measured NPP in the Bukit Duabelas landscape is 10% higher than that in the Harapan landscape
420 (Kotowska et al., 2015), and (2) the amount of measured latex yield was also higher in the Bukit
421 Duabelas landscape than the Harapan landscape (Kotowska et al., 2015), although it was not
422 statistically different. To save space, we include figures for the model calibration in the main
423 manuscript and put figures for the model validation in the supplementary section.

424

425 *Hypothesis testing*



426 Understanding tropical droughts is important because it affects the growth and mortality
427 of trees (e.g. Bretfeld et al., 2018; Moser et al., 2014; Phillips et al., 2010). Sometimes drought
428 can be really hard on forests, where too much heat, low humidity and not enough water can
429 drastically alter which trees survive (Lewis et al., 2011; Rowland et al., 2015). In the future,
430 drought is projected to increase (Jiménez-Muñoz et al., 2016; Neelin et al., 2006); however, our
431 ability to predict how future dry conditions would impact rubber tree productivity and yield is
432 limited. Therefore, we used CLM-rubber to investigate the impacts of future drought on rubber
433 yield. We expected drought to reduce the productivity of rubber trees in addition to the latex
434 yield. We focused on five low rainfall scenarios; two simulations assumed low rainfall to occur
435 throughout the year and so these simulations had 20%, 50% lower precipitation than the default
436 precipitation; the other two simulations assumed low rainfall to occur with the extended dry
437 season and so precipitation from April to October was reduced by 30%, 50%, in these
438 simulations; and the final simulation considered shorter dry season but with intense drought so in
439 this simulation precipitation from 8th May to 12th September was reduced by 50%. We then
440 performed six simulations of 10-year period from 2015 to 2024; first using the present-day
441 climate data, and then for the other five simulations, we used the climate data that imposed
442 drying.

443

444 *Leaf life span and specific leaf area*

445 In the current version of the CLM-rubber, specific leaf area (SLA) is fixed; which is the
446 case for many land surface models. It has been suggested that SLA could decline with leaf age
447 e.g. due to leaf economics. We do not have temporal data on SLA for rubber. Because we
448 developed a rubber model where we included the temporal changes in leaf life span for better
449 model fit to the leaf litterfall data, we decided to investigate the effect of a dynamic SLA on the
450 modeled photosynthesis of the rubber at the leaf-level. In CLM4.5 as well as in CLM-rubber,
451 SLA is referred to as “slatop” – the SLA at the top of the canopy. To have a dynamic SLA, we
452 let SLA to be low when the leaf life span is relatively high and SLA to be high when leaf life
453 span is relatively low. The leaf life span is high in the wet than the dry season. We used a
454 calendar month-dependent function to model the dynamics of slatop:

$$455 \quad \text{slatop} = \begin{cases} 0.0197, & \text{month} \leq 5 \\ 0.024, & 6 \leq \text{month} \leq 9 \\ 0.0197, & \text{month} > 9 \end{cases} \quad (12)$$



456 In Eq. 12, slatop is low in the wet than the dry season, where we reduced slatop by 18% in the
457 wet season.

458

459 *Comparison with other models and locations*

460 We do not have a flux-net tower in the rubber plantations in Jambi, Indonesia. However,
461 the CLM-rubber model has been calibrated to carbon and water flux related variables for rubber
462 plantations at Jambi, Indonesia. Therefore, we think that the modeled estimates of carbon and
463 water fluxes of CLM-rubber at Jambi, Indonesia can be considered as a “proxy” of measured
464 fluxes of rubber plantation in Jambi, Indonesia. Thus, we have an opportunity now to compare
465 modeled estimates of carbon and water fluxes of CLM-rubber in Jambi, Indonesia with
466 measurements of fluxes from two rubber plantations at other locations in the Southeast Asia
467 (Giambelluca et al., 2016). To check the robustness of the CLM-rubber in prediction of the water
468 fluxes, we compared its modeled water fluxes with the predicted values from a soil water model
469 (Kurniawan et al., 2018), that is parameterized with the site-specific soil physical and
470 hydrological parameters from our studied plots. Finally, to identify the relative ranking of the
471 above-ground carbon stock of rubber plantations, we compared the measured and modeled
472 estimates of carbon from our site in Jambi province, Indonesia with measurements from China,
473 Africa and Brazil (Kotowska et al., 2015; Wauters et al., 2008; Yang et al., 2016).

474

475 **Results**

476 *Dynamics of carbon use*

477 CLM-rubber was able to simulate the dynamics of net primary productivity (Figure 2; a),
478 above-ground biomass (Figure 2; b) and total soil organic carbon (Figure 2; c) of the rubber
479 plantation in the Harapan landscape. The modeled biomass of fine roots and the annual latex
480 yield were also within the measured range (Figure 3; a, b). When validated in the Bukit Duabelas
481 landscape, the modeled net primary productivity (Figure S2; a) and above ground biomass
482 (Figure S2; b) were quite close to the measurements. The modeled biomass of the fine roots and
483 the annual latex yield were much closer to the measurements in the model validation case
484 (Figure S3; a, b) than the model calibration case (Figure 3; a, b).



485 Despite the large variability across plots for the measured values, CLM-rubber captured
486 the seasonal dynamics of the leaf litterfall (Figure 4a) far better than the seasonal trends of soil
487 respiration (Figure 4b) and soil moisture (Figure 4c) in the Harapan landscape. For leaf area
488 index, the measured values in 2018 were below our simulated values for 2014 (Figure 4d); there
489 may be also an inter-annual variability of leaf area index, aside from seasonal variability, since
490 for the leaf litterfall to be captured well by the CLM-rubber the LAI must be predicted
491 reasonably well for 2014. The modeled seasonal patterns of carbon and water dynamics at the
492 Bukit Duabelas landscape (Figure S4) were similar with those at the Harapan landscape.

493

494 *Dynamics of water use*

495 The calibrated model in the Harapan landscape was close to the pattern and magnitude of
496 the measured diel transpiration in a dry (Figure 5; a) and wet month (Figure 5; b). The modeled
497 and measured diel courses of transpiration were characterized by relatively low hourly maxima
498 ($< 0.25 \text{ mm h}^{-1}$; Figure 5). The model had an early onset as well as an early offset of
499 transpiration than the measurements (Figure 5; a, b). This is consistent with the diurnal effects
500 that nitrogen limitation is known to have in CLM4.5 (see Fig.1; Ghimire et al., 2016). The model
501 successfully predicted the average transpiration of a 2-year and 5-year old rubber plantations
502 (Figure 6; a, b).

503 The validated results in the Bukit Duabelas landscape showed that the diel trends of
504 predicted and measured transpiration were quite similar (Figure S5; a-c) to those in the Harapan
505 landscape. The model captured the long-term seasonal trends of transpiration well (Figure S6),
506 except for a minor discrepancy for a few weeks in June, where there was some period of partial
507 leaf shedding. The magnitude of the modeled transpiration was also quite close to the
508 measurements (Figure S6).

509

510 *Leaf life span and specific leaf area*

511 Since in the CLM-rubber the trees have a drought-deciduous leaf phenology, we
512 investigated the effect of fixed versus dynamic specific leaf area (Figure 7; a, b) and found that
513 the mass-based photosynthesis of rubber leaves had a stronger dependence on leaf life span when
514 the specific leaf area is dynamic (a higher r^2 value; Figure 7; b) rather than fixed. Interestingly,



515 the model predicted that a higher mass-based photosynthesis of the rubber leaf can be associated
516 with a lower leaf life span - this is a proposition that cannot be drawn if the specific leaf area is
517 fixed (i.e. Figure 7; a). This finding suggests that long-lived rubber leaves could have a low
518 mass-based photosynthesis, and that rubber plants could spend carbon in the construction of
519 other tissues such as those associated with protection against insects or prevention of leaf
520 diseases.

521

522 *Model Projection*

523 CLM-rubber predicted reduced yield in response to different drought scenarios as the
524 intensity of drought increased (Figure 8). Modeled yield tended to have a non-linear relationship
525 with soil moisture. CLM-rubber predicted up to a 18% reduction in yield when the intensity and
526 duration of drought was largest (Figure 8). Currently, we do not have field data to confirm the
527 magnitude of the effect of drought on yield, predicted by the model.

528

529 *Comparison with other sites and models*

530 CLM-rubber predicted a lower carbon uptake in the wettest month for Jambi, Indonesia
531 compared to measurements of a similar plantation from Thailand (Table 1). The model also
532 predicted a lower carbon release in the driest month for Jambi than a similar plantation from
533 Thailand (Table 1). It should be pointed out that the rubber plantations in Jambi were unfertilized
534 in the recent years and are on highly weathered Acrisol soils with low fertility while the rubber
535 plantation in Thailand are highly fertilized. The CLM-rubber carbon fluxes suggest that rubber
536 plantations from our sites are unlikely to have high carbon uptake or releases at the ecosystem
537 scale compared to rubber plantations from other parts of Asia because the rubber plantations
538 from our sites are not fertilized and have low leaf area index. At the ecosystem scale, CLM-
539 rubber predicted a lower annual evapotranspiration and higher sensible heat fluxes from our sites
540 than a similar plantation from Thailand (Table 1). These results indicate that rubber plantations
541 from our sites are likely to have a high canopy openness than rubber plantations from other parts
542 of Asia.

543 The comparison of water fluxes of CLM-rubber with a site-parameterized soil water
544 model showed that CLM-rubber can predict the water fluxes reasonably well (Table 2). When
545 comparing the carbon stocks of Jambi, Indonesia with other tropical countries, we found that the



546 above-ground biomass of rubber plantations was mostly similar except for a plantation from
547 Africa (Table 3).

548

549 **Discussion**

550 *Phenology and Carbon & Nitrogen Allocation*

551 The seasonality observed in the empirical leaf litterfall data represented a challenge for
552 the development of the CLM-rubber. During CLM-rubber development, we realized that the
553 version of CLM-rubber that did not consider the temporal changes in leaf life span (that had
554 fixed leaf life span as 1 year) failed to capture the seasonality of leaf litterfall. We have
555 demonstrated in this study the importance of temporal changes in leaf life span. Seasonal data on
556 leaf life span and leaf area index for rubber trees will be invaluable to capture well the carbon
557 cycle of CLM-rubber. Similar data sets for tropical deciduous trees should be collected, which
558 currently are rare (Dahlin et al., 2017). Our study suggests that land surface models should not
559 use fixed leaf life span for simulating carbon dynamics of tropical deciduous PFTs if the focus of
560 the study is examining seasonal pattern.

561 Radiation intensity has been suggested to play an important role in the onset of rubber
562 leaves for the sub-tropics (Hoong-Yeet, 2007). At this stage, we did not integrate radiation
563 intensity to trigger the onset of rubber leaves in the CLM-rubber because we do not have
564 sufficient phenology data. Currently, the trigger for leaf onset in CLM-rubber is based on soil
565 water potential. The carbon cycle of CLM-rubber can therefore be further improved by
566 examining possible controls on leaf shedding and flushing in rubber and their interactions, e.g.
567 soil water potential and radiation intensity.

568 The seemingly higher latex yield of rubber plantation in the Bukit Duabelas landscape
569 compared to the Harapan landscape (despite being five years younger than Harapan) could be
570 due to differences in management practices between the two landscapes (e.g. tapping frequency,
571 planting density; Kotowska et al., 2015) and/or differences in soil texture, which influences
572 differences in fertility (Allen et al., 2016; Allen et al., 2015; Kurniawan et al., 2018). The change
573 in Q10 value of soil temperature enabled CLM-rubber to predict a 16% decline in soil carbon
574 since clear-cut – a finding that is similar to a study by van Straaten et al. (2015). Indeed, in a



575 recent study, Meyer et al. (2018) have shown that Q10 has a lot of variability across PFTs,
576 ranging from 1.25 to 2.75.

577

578 *Low transpiration rates*

579 The inclusion of increased sensitivity of stomata to soil water stress and the enhancement
580 of growth and maintenance respiration of fine roots in response to soil nutrient limitation enabled
581 CLM-rubber to capture the magnitude of transpiration and leaf area index; however, the model
582 had an earlier onset of diel transpiration (Figure 5; a, b) as well as an earlier offset of
583 transpiration (Figure 5; a, b) than the measurements. The early onset of modeled transpiration
584 around 8 am can be explained by the relatively high radiation (Figure S7; a) while the early
585 offset of modeled transpiration around 6 pm (Figure 5; a) can be related to the absence of the
586 stem water storage term in the model. The sap flow measurements could also have uncertainties
587 due to their set-up. The sensors were inserted in the tree trunk at about 2 m height. Above this
588 height, there could be considerable water storage in the plant. Early in the morning, transpiration
589 may make use of this water storage – as indicated by the modeled transpiration. In the evening,
590 the plant water storage above the sap flow sensors may be refilled, and thus water flow at the
591 trunk is measured. Another source of error in the measurements of transpiration can be related to
592 the fact that there were only 5 sap flow sensors, which were then used to upscale transpiration to
593 the canopy-level.

594 CLM-rubber showed that rubber plantations can exhibit two peaks of leaf photosynthesis
595 during a day (Figure S8; a), which could be due to the existence of optimal climatic conditions
596 operating at multiple times within a day (Figure S7; a-c). Although absorbed PAR remained
597 relatively high around noon time (Figure S8; b), the modeled leaf photosynthesis declined due to
598 limitations in soil water and stomatal conductance (Figure S8; a). The model simulated the long-
599 term dynamics of transpiration close to measurements (Niu et al., 2017). Our results are not
600 consistent with reports speculating that rubber trees could be large carbon sinks (Kumagai et al.,
601 2013) and behave as ‘water pumps’ (Tan et al., 2011; Ziegler et al., 2012).

602 Other factors such as carbon economy, plant health and soil degradation (Sitorus and
603 Pravitasari, 2017) could also constrain the productivity and water use of rubber at our studied
604 sites. CLM-rubber clearly provides additional opportunities to test hypotheses of the effects of



605 climate scenarios, management practices to alleviate nutrient limitations or their combinations on
606 carbon economy of rubber plantations.

607

608 *Dynamic traits & uncertainties in leaf area index*

609 From this CLM-rubber development, we can derive suggestions for improving current
610 land surface models. While the carbon, water and nutrient cycles in land surface models have
611 improved considerably, the development of trees from seedlings to mature growth phases is less
612 well represented (Fisher et al., 2018). Our model clearly demonstrates that some of the basic
613 plant functional traits, e.g. leaf life span, even specific leaf area that are currently considered
614 fixed parameters in land surface models, need a dynamic seasonal component (Girardin et al.,
615 2016; Lopes et al., 2016; Wu et al., 2016). This may further apply for longer-term dynamics, e.g.
616 with regards to different growth phases. Follow-up research is needed to align seasonal and
617 growth phase-related plant traits, e.g. leaf life span, fruiting of rubber trees, and leaf area index.

618 From a theoretical point of view, very young and old leaves are unlikely to have a mass-
619 based photosynthetic rate as high as that of fully expanded mature leaves. Broadly, this finding
620 has some support from tropical studies (Albert et al., 2018) but needs to be evaluated for rubber.

621 The fact that CLM-rubber did not capture the magnitude of the measured leaf area index
622 in 2018 (measured with a LAI 2000 measurements, LiCor Biosciences Inc.) can be due to large
623 variability in climatic factors, such as flux density of photosynthetically active radiation as well
624 as the time of measurement (Cotter et al., 2017). We also obtained leaf area index for year 2014
625 from MODIS satellite on clear sky days for the studied rubber plantations. The MODIS leaf area
626 index was as high as $4 \text{ m}^2 \text{ m}^{-2}$, which is similar to the predictions of CLM-rubber.

627

628 *Opportunities for CLM-rubber*

629 As CLM-rubber predicted reasonably well the carbon and water use, we think that the
630 current model can be used for larger-scale simulations within Indonesia, in particular, the
631 lowland areas with mineral soils of Jambi province by incorporating in the prediction soil texture
632 as the surrogate variable for the control of soil fertility and soil moisture. CLM-rubber can aid in
633 science-based management and policy recommendations, as the model can be applied to
634 scenarios of soil management intensities, climate variations, and policy-driven land-use change



635 projections. CLM-rubber model can also be applied to rubber plantations in other regions in
636 Southeast Asia but it will require validation against measured carbon, water and energy flux data
637 from the Asia flux community (Giambelluca et al., 2016; Kumagai et al., 2013; Tan et al., 2011).

638 Plot-level simulations can potentially be performed for so called jungle rubber plantations
639 (Feintrenie and Levang, 2009; Gouyon et al., 1993), where the rubber and the trees from the
640 natural tropical forest coexist. Here, we can use the newly developed CLM-FATES model,
641 which has a demographic component that considers processes such as height-structured
642 vegetation and competition between individuals for light (Fisher et al., 2015). In Jambi province,
643 jungle rubber represents a smallholder rubber agroforestry system, which is established by
644 planting rubber trees into (often previously logged) rainforests. Similar measured data used in the
645 current study exists for eight jungle rubber plots differing in soil texture, nutrient levels and
646 water characteristics. The abundance of natural and rubber trees need to be incorporated in the
647 model and then carbon and water cycles can be investigated.

648 Additional experimental data in the dry season on leaf aging and fruiting of rubber should
649 be collected to investigate if rubber plants take advantage of the high light availability, while
650 coping with high atmospheric water demand and low water supply. These empirical data can be
651 an indicator of adaptive strategies of how rubber plants optimize reproduction and resource
652 acquisition.

653

654 **Final Remarks**

655 Incorporating a dynamic leaf life span enabled CLM-rubber to better capture the
656 seasonality of leaf litterfall. Increased sensitivity of stomata to soil water stress and the
657 enhancement of growth and maintenance respiration of fine roots in response to soil nutrient
658 limitation enabled CLM-rubber to capture the magnitude of transpiration and leaf area index.
659 Our results show that rubber plantations in Jambi are less likely to have similarly high carbon
660 fluxes and water use compared to highly fertilized rubber plantations from other parts of South-
661 east Asia such as those from Thailand and Cambodia.

662

663

664



665 **Code & Data Availability**

666 Code is available on GitHub (https://github.com/ashehad/CLM4.5_rubber_v1/tree/master/codes)
667 and data used in this paper can be found in this repository
668 (https://github.com/ashehad/CLM4.5_rubber_v1/tree/master/data/measured_data_for_model_calibration).
669
670

671 **Acknowledgements**

672 We gratefully acknowledge financial supports from Deutsche Forschungsgemeinschaft (DFG) in
673 the framework of the collaborative German-Indonesian research project CRC990 in subproject
674 A07. We thank Syahrul Kurniawan for running the soil-water model and Aiyen Tjoa from the
675 University of Jambi (UNJA), Jambi, Indonesia for taking canopy pictures of rubber plantations
676 during the dry season. Katie Dagon from National Center for Atmospheric Research is thanked
677 for discussing the hydrological processes in CLM4.5. We also thank George Ofori Ankomah
678 from the University of Goettingen for measuring the leaf area index at the studied rubber
679 plantations. Finally, we thank the village leaders, PT REKI and Bukit Duabelas National Park for
680 allowing us to conduct our research on their land.
681
682
683

684 **References**

685 Albert, L. P., Wu, J., Prohaska, N., Camargo, P. B., Huxman, T. E., Tribuzy, E. S., Ivanov, V.
686 Y., Oliveira, R. S., Garcia, S., Smith, M. N., Oliveira, J. R. C., Restrepo-Coupe, N., Silva, R.,
687 Stark, S. C., Martins, G. A., Penha, D. V., and Saleska, S. R.: Age-dependent leaf physiology
688 and consequences for crown-scale carbon uptake during the dry season in an Amazon evergreen
689 forest, *New Phytologist*, 219, 870-884, 2018.
690 Ali, A. A., Xu, C., Rogers, A., Fisher, R. A., Wullschleger, S. D., Massoud, E. C., Vrugt, J. A.,
691 Muss, J. D., McDowell, N. G., Fisher, J. B., Reich, P. B., and Wilson, C. J.: A global scale
692 mechanistic model of photosynthetic capacity (LUNA V1.0) *Geosci. Model Dev.*, 9, 587-606,
693 2016.



- 694 Allen, K., Corre, M. D., Kurniawan, S., Utami, S. R., and Veldkamp, E.: Spatial variability
695 surpasses land-use change effects on soil biochemical properties of converted lowland
696 landscapes in Sumatra, Indonesia, *Geoderma*, 284, 42-50, 2016.
- 697 Allen, K., Corre, M. D., Tjoa, A., and Veldkamp, E.: Soil Nitrogen-Cycling Responses to
698 Conversion of Lowland Forests to Oil Palm and Rubber Plantations in Sumatra, Indonesia, *PLoS*
699 *ONE*, 10, e0133325, 2015.
- 700 Blagodatsky, S., Xu, J., and Cadisch, G.: Carbon balance of rubber (*Hevea brasiliensis*)
701 plantations: A review of uncertainties at plot, landscape and production level, *Agriculture,*
702 *Ecosystems & Environment*, 221, 8-19, 2016.
- 703 Boisier, J. P., Noblet-Ducoudré, N., Pitman, A. J., Cruz, F. T., Delire, C., den Hurk, B. J. J. M.,
704 Molen, M. K., Müller, C., and Voltaire, A.: Attributing the impacts of land-cover changes in
705 temperate regions on surface temperature and heat fluxes to specific causes: Results from the
706 first LUCID set of simulations, *Journal of Geophysical Research: Atmospheres*, 117, 2012.
- 707 Bonan, G. B. and Doney, S. C.: Climate, ecosystems, and planetary futures: The challenge to
708 predict life in Earth system models, *Science*, 359, 2018.
- 709 Bonan, G. B., Levis, S., Kergoat, L., and Oleson, K. W.: Landscapes as patches of plant
710 functional types: An integrating concept for climate and ecosystem models, *Global*
711 *Biogeochemical Cycles*, 16, 5-1-5-23, 2002.
- 712 Bretfeld, M., Ewers, B. E., and Hall, J. S.: Plant water use responses along secondary forest
713 succession during the 2015–2016 El Niño drought in Panama, *New Phytologist*, 219, 885-899,
714 2018.
- 715 Carr, M. K. V.: THE WATER RELATIONS OF RUBBER (*HEVEA BRASILIENSIS*): A
716 REVIEW, *Experimental Agriculture*, 48, 176-193, 2012.
- 717 Chantuma, P., Lacoïnte, A., Kasemsap, P., Thanisawanyangkura, S., Gohet, E., Clément, A.,
718 Guillot, A., Améglio, T., and Thaler, P.: Carbohydrate storage in wood and bark of rubber trees
719 submitted to different level of C demand induced by latex tapping, *Tree Physiology*, 29, 1021-
720 1031, 2009.
- 721 Corre, M. D., Dechert, G., and Veldkamp, E.: Soil Nitrogen Cycling following Montane Forest
722 Conversion in Central Sulawesi, Indonesia, *Soil Science Society of America Journal*, 70, 359-
723 366, 2006.



- 724 Cotter, M., Asch, F., Hilger, T., Rajaona, A., Schappert, A., Stuerz, S., and Yang, X.: Measuring
725 leaf area index in rubber plantations – a challenge, *Ecological Indicators*, 82, 357-366, 2017.
- 726 Dahlin, K. M., Del Ponte, D., Setlock, E., and Nagelkirk, R.: Global patterns of drought
727 deciduous phenology in semi-arid and savanna-type ecosystems, *Ecography*, 40, 314-323, 2017.
- 728 Dahlin, K. M., Fisher, R. A., and Lawrence, P. J.: Environmental drivers of drought deciduous
729 phenology in the Community Land Model, *Biogeosciences*, 12, 5061-5074, 2015.
- 730 de Blécourt, M., Brumme, R., Xu, J., Corre, M. D., and Veldkamp, E.: Soil Carbon Stocks
731 Decrease following Conversion of Secondary Forests to Rubber (*Hevea brasiliensis*) Plantations,
732 *PLoS ONE*, 8, e69357, 2013.
- 733 Doughty, C. E., Goldsmith, G. R., Raab, N., Girardin, C. A. J., Farfan-Amezquita, F., Huaraca-
734 Huasco, W., Silva-Espejo, J. E., Araujo-Murakami, A., Costa, A. C. L., Rocha, W., Galbraith,
735 D., Meir, P., Metcalfe, D. B., and Malhi, Y.: What controls variation in carbon use efficiency
736 among Amazonian tropical forests?, *Biotropica*, 50, 16-25, 2018.
- 737 Drescher, J., Rembold, K., Allen, K., Beckschäfer, P., Buchori, D., Clough, Y., Faust, H., Fauzi,
738 A. M., Gunawan, D., Hertel, D., Irawan, B., Jaya, I. N. S., Klarner, B., Kleinn, C., Knohl, A.,
739 Kotowska, M. M., Krashevskaya, V., Krishna, V., Leuschner, C., Lorenz, W., Meijide, A., Melati,
740 D., Nomura, M., Pérez-Cruzado, C., Qaim, M., Siregar, I. Z., Steinebach, S., Tjoa, A.,
741 Tschardtke, T., Wick, B., Wiegand, K., Kreft, H., and Scheu, S.: Ecological and socio-economic
742 functions across tropical land use systems after rainforest conversion, *Philosophical Transactions*
743 *of the Royal Society B: Biological Sciences*, 371, 20150275, 2016.
- 744 Eleanor, W.-T., M., D. P., and P., E. D.: Increasing Demand for Natural Rubber Necessitates a
745 Robust Sustainability Initiative to Mitigate Impacts on Tropical Biodiversity, *Conservation*
746 *Letters*, 8, 230-241, 2015.
- 747 Fan, Y., Rounsard, O., Bernoux, M., Le Maire, G., Panferov, O., Kotowska, M. M., and Knohl,
748 A.: A sub-canopy structure for simulating oil palm in the Community Land Model (CLM-Palm):
749 phenology, allocation and yield, *Geosci. Model Dev.*, 8, 3785-3800, 2015.
- 750 Feintrenie, L. and Levang, P.: Sumatra's Rubber Agroforests: Advent, Rise and Fall of a
751 Sustainable Cropping System, *Small-scale Forestry*, 8, 323-335, 2009.
- 752 Fisher, J. B., Sweeney, S., Brzostek, E. R., Evans, T. P., Johnson, D. J., Myers, J. A., Bourg, N.
753 A., Wolf, A. T., Howe, R. W., and Phillips, R. P.: Tree-mycorrhizal associations detected
754 remotely from canopy spectral properties, *Global Change Biology*, 22, 2596-2607, 2016.



- 755 Fisher, R. A., Koven, C. D., Anderegg, W. R. L., Christoffersen, B. O., Dietze, M. C., Farrior, C.
756 E., Holm, J. A., Hurtt, G. C., Knox, R. G., Lawrence, P. J., Lichstein, J. W., Longo, M.,
757 Matheny, A. M., Medvigy, D., Muller-Landau, H. C., Powell, T. L., Serbin, S. P., Sato, H.,
758 Shuman, J. K., Smith, B., Trugman, A. T., Viskari, T., Verbeeck, H., Weng, E., Xu, C., Xu, X.,
759 Zhang, T., and Moorcroft, P. R.: Vegetation demographics in Earth System Models: A review of
760 progress and priorities, *Global Change Biology*, 24, 35-54, 2018.
- 761 Fisher, R. A., Muszala, S., Versteinstein, M., Lawrence, P., Xu, C., McDowell, N. G., Knox, R.
762 G., Koven, C., Holm, J., Rogers, B. M., Spessa, A., Lawrence, D., and Bonan, G.: Taking off the
763 training wheels: the properties of a dynamic vegetation model without climate envelopes,
764 *CLM4.5(ED)*, *Geosci. Model Dev.*, 8, 3593-3619, 2015.
- 765 Gellert, P. K.: The Shifting Natures of “Development”: Growth, Crisis, and Recovery in
766 Indonesia’s Forests, *World Development*, 33, 1345-1364, 2005.
- 767 Ghimire, B., Riley, W. J., Koven, C. D., Mu, M., and Randerson, J. T.: Representing leaf and
768 root physiological traits in CLM improves global carbon and nitrogen cycling predictions,
769 *Journal of Advances in Modeling Earth Systems*, 8, 598-613, 2016.
- 770 Giambelluca, T. W., Mudd, R. G., Liu, W., Ziegler, A. D., Kobayashi, N., Kumagai, T. o.,
771 Miyazawa, Y., Lim, T. K., Huang, M., Fox, J., Yin, S., Mak, S. V., and Kasemsap, P.:
772 Evapotranspiration of rubber (*Hevea brasiliensis*) cultivated at two plantation sites in Southeast
773 Asia, *Water Resources Research*, 52, 660-679, 2016.
- 774 Girardin, C. A. J., Malhi, Y., Doughty, C. E., Metcalfe, D. B., Meir, P., Aguila-Pasquel, J.,
775 Araujo-Murakami, A., Costa, A. C. L., Silva-Espejo, J. E., Farfán Amézquita, F., and Rowland,
776 L.: Seasonal trends of Amazonian rainforest phenology, net primary productivity, and carbon
777 allocation, *Global Biogeochemical Cycles*, 30, 700-715, 2016.
- 778 Gouyon, A., de Foresta, H., and Levang, P.: Does ‘jungle rubber’ deserve its name? An analysis
779 of rubber agroforestry systems in southeast Sumatra, *Agroforestry Systems*, 22, 181-206, 1993.
- 780 Granier, A.: Une nouvelle méthode pour la mesure du flux de sève brute dans le tronc des arbres,
781 *Ann. For. Sci.*, 42, 193-200, 1985.
- 782 Hanna, P., A., V. J., Andrew, F., Harry, V., and Harrie-Jan, H. F.: Estimation of Community
783 Land Model parameters for an improved assessment of net carbon fluxes at European sites,
784 *Journal of Geophysical Research: Biogeosciences*, 122, 661-689, 2017.



- 785 Hassler, E., Corre, M. D., Tjoa, A., Damris, M., Utami, S. R., and Veldkamp, E.: Soil fertility
786 controls soil–atmosphere carbon dioxide and methane fluxes in a tropical landscape converted
787 from lowland forest to rubber and oil palm plantations, *Biogeosciences*, 12, 5831-5852, 2015.
- 788 Hoong-Yeet, Y.: Synchronous flowering of the rubber tree (*Hevea brasiliensis*) induced by high
789 solar radiation intensity, *New Phytologist*, 175, 283-289, 2007.
- 790 Houghton, R. A., House, J. I., Pongratz, J., van der Werf, G. R., DeFries, R. S., Hansen, M. C.,
791 Le Quéré, C. C., and Ramankutty, N.: Carbon emissions from land use and land-cover change,
792 *Biogeosciences*, 9, 5125-5142, 2012.
- 793 Jiménez-Muñoz, J. C., Mattar, C., Barichivich, J., Santamaría-Artigas, A., Takahashi, K., Malhi,
794 Y., Sobrino, J. A., and Schrier, G. v. d.: Record-breaking warming and extreme drought in the
795 Amazon rainforest during the course of El Niño 2015–2016, *Scientific Reports*, 6, 33130, 2016.
- 796 Junjittakarn, J., Liminuntana, V., Pannengetch, K., Ayutthaya, S. I. N., Rocheteau, A., Cochard,
797 H., and Frédéric, D.: Short term effects of latex tapping on micro-changes of trunk girth in *Hevea*
798 *brasiliensis*, *Australian Journal of Crop Science*, 6, 65-72, 2012.
- 799 Kotowska, M. M., Leuschner, C., Triadiati, T., and Hertel, D.: Conversion of tropical lowland
800 forest reduces nutrient return through litterfall, and alters nutrient use efficiency and seasonality
801 of net primary production, *Oecologia*, 180, 601-618, 2016.
- 802 Kotowska, M. M., Leuschner, C., Triadiati, T., Meriem, S., and Hertel, D.: Quantifying above-
803 and belowground biomass carbon loss with forest conversion in tropical lowlands of Sumatra
804 (Indonesia), *Global Change Biology*, 21, 3620-3634, 2015.
- 805 Koven, C. D., Riley, W. J., Subin, Z. M., Tang, J. Y., Torn, M. S., Collins, W. D., Bonan, G. B.,
806 Lawrence, D. M., and Swenson, S. C.: The effect of vertically resolved soil biogeochemistry and
807 alternate soil C and N models on C dynamics of CLM4, *Biogeosciences*, 10, 7109-7131, 2013.
- 808 Kumagai, T., Mudd, R. G., Miyazawa, Y., Liu, W., Giambelluca, T. W., Kobayashi, N., Lim, T.
809 K., Jomura, M., Matsumoto, K., Huang, M., Chen, Q., Ziegler, A., and Yin, S.: Simulation of
810 canopy CO₂/H₂O fluxes for a rubber (*Hevea brasiliensis*) plantation in central Cambodia: The
811 effect of the regular spacing of planted trees., *Ecological Modelling*, 265, 124-135, 2013.
- 812 Kurniawan, S., Corre, M. D., Matson, A. L., Schulte-Bisping, H., Utami, S. R., van Straaten, O.,
813 and Veldkamp, E.: Conversion of tropical forests to smallholder rubber and oil palm plantations
814 impacts nutrient leaching losses and nutrient retention efficiency in highly weathered soils,
815 *Biogeosciences*, 5131-5154, 2018.



- 816 Lewis, S. L., Brando, P. M., Phillips, O. L., van der Heijden, G. M. F., and Nepstad, D.: The
817 2010 Amazon Drought, *Science*, 331, 554-554, 2011.
- 818 Lin, Y., Zhang, Y., Zhao, W., Dong, Y., Fei, X., Song, Q., Sha, L., Wang, S., and Grace, J.:
819 Pattern and driving factor of intense defoliation of rubber plantations in SW China, *Ecological*
820 *Indicators*, 94, 104-116, 2018.
- 821 Lopes, A. P., Nelson, B. W., Wu, J., Graça, P. M. L. d. A., Tavares, J. V., Prohaska, N., Martins,
822 G. A., and Saleska, S. R.: Leaf flush drives dry season green-up of the Central Amazon, *Remote*
823 *Sensing of Environment*, 182, 90-98, 2016.
- 824 Maite, G.-C., A., T. P., D., Z. A., W., G. T., B., V. J., and A., N. M.: Local hydrologic effects of
825 introducing non-native vegetation in a tropical catchment, *Ecohydrology*, 1, 13-22, 2008.
- 826 Mann, C. C.: Addicted to Rubber, *Science*, 325, 564-566, 2009.
- 827 Margono, B. A., Turubanova, S., Zhuravleva, I., Potapov, P., Tyukavina, A., Baccini, A., Goetz,
828 S., and Hansen, M. C.: Mapping and monitoring deforestation and forest degradation in Sumatra
829 (Indonesia) using Landsat time series data sets from 1990 to 2010, *Environmental Research*
830 *Letters*, 7, 034010, 2012.
- 831 Medlyn, B. E., De Kauwe, M. G., and Duursma, R. A.: New developments in the effort to model
832 ecosystems under water stress, *New Phytologist*, 212, 5-7, 2016.
- 833 Meijide, A., Badu, C. S., Moyano, F., Tiralla, N., Gunawan, D., and Knohl, A.: Impact of forest
834 conversion to oil palm and rubber plantations on microclimate and the role of the 2015 ENSO
835 event, *Agricultural and Forest Meteorology*, 252, 208-219, 2018.
- 836 Melati, D.: Land Use Cover, PhD Thesis, Remote Sensing, University of Goettingen, Germany,
837 Goettingen, 2017.
- 838 Meyer, N., Welp, G., and Amelung, W.: The Temperature Sensitivity (Q₁₀) of Soil Respiration:
839 Controlling Factors and Spatial Prediction at Regional Scale Based on Environmental Soil
840 Classes, *Global Biogeochemical Cycles*, 32, 306-323, 2018.
- 841 Moser, G., Schuldt, B., Hertel, D., Horna, V., Coners, H., Barus, H., and Leuschner, C.:
842 Replicated throughfall exclusion experiment in an Indonesian perhumid rainforest: wood
843 production, litter fall and fine root growth under simulated drought, *Global Change Biology*, 20,
844 1481-1497, 2014.
- 845 Nadezhdina, N., Vandegehuchte, M. W., and Steppe, K.: Sap flux density measurements based
846 on the heat field deformation method, *Trees*, 26, 1439-1448, 2012.



- 847 Neelin, J. D., Münnich, M., Su, H., Meyerson, J. E., and Holloway, C. E.: Tropical drying trends
848 in global warming models and observations, *Proceedings of the National Academy of Sciences*,
849 103, 6110-6115, 2006.
- 850 Niu, F., Röhl, A., Meijide, A., Hendrayanto, and Hölscher, D.: Rubber tree transpiration in the
851 lowlands of Sumatra, *Ecohydrology*, 10, e1882-n/a, 2017.
- 852 Oleson, K. W., Lawrence, D. M., Bonan, G. B., Drewniak, B., Huang, M., Koven, C. D., Levis,
853 S., Li, F., Riley, W. J., Subin, Z. M., Swenson, S. C., Thornton, P. E., Bozbiyik, A., Fisher, R.,
854 Kluzek, E., Lamarque, J.-F., Lawrence, P. J., Leung, L. R., Lipscomb, W., Muszala, S., Ricciuto,
855 D. M., Sacks, W., Sun, Y., Tang, J., and Yang, Z.-L.: Technical Description of version 4.5 of the
856 Community Land Model (CLM). NCAR Technical Note NCAR/TN-503+STR, National Center
857 for Atmospheric Research, Boulder, CO, 2013.
- 858 Phillips, O. L., van der Heijden, G., Lewis, S. L., López-González, G., Aragão, L. E. O. C.,
859 Lloyd, J., Malhi, Y., Monteagudo, A., Almeida, S., Dávila, E. A., Amaral, I., Andelman, S.,
860 Andrade, A., Arroyo, L., Aymard, G., Baker, T. R., Blanc, L., Bonal, D., de Oliveira, Á. C. A.,
861 Chao, K.-J., Cardozo, N. D., da Costa, L., Feldpausch, T. R., Fisher, J. B., Fyllas, N. M., Freitas,
862 M. A., Galbraith, D., Gloor, E., Higuchi, N., Honorio, E., Jiménez, E., Keeling, H., Killeen, T. J.,
863 Lovett, J. C., Meir, P., Mendoza, C., Morel, A., Vargas, P. N., Patiño, S., Peh, K. S.-H., Cruz, A.
864 P., Prieto, A., Quesada, C. A., Ramírez, F., Ramírez, H., Rudas, A., Salamão, R., Schwarz, M.,
865 Silva, J., Silveira, M., Ferry Slik, J. W., Sonké, B., Thomas, A. S., Stropp, J., Taplin, J. R. D.,
866 Vásquez, R., and Vilanova, E.: Drought–mortality relationships for tropical forests, *New*
867 *Phytologist*, 187, 631-646, 2010.
- 868 Pitman, A. J., de Noblet-Ducoudré, N., Cruz, F. T., Davin, E. L., Bonan, G. B., Brovkin, V.,
869 Claussen, M., Delire, C., Ganzeveld, L., Gayler, V., van den Hurk, B. J. J. M., Lawrence, P. J.,
870 van der Molen, M. K., Müller, C., Reick, C. H., Seneviratne, S. I., Strengers, B. J., and Voldoire,
871 A.: Uncertainties in climate responses to past land cover change: First results from the LUCID
872 intercomparison study, *Geophysical Research Letters*, 36, 2009.
- 873 Powers, J. S., Corre, M. D., Twine, T. E., and Veldkamp, E.: Geographic bias of field
874 observations of soil carbon stocks with tropical land-use changes precludes spatial extrapolation,
875 *Proceedings of the National Academy of Sciences*, 108, 6318-6322, 2011.
- 876 Qui, J.: Where the rubber meets the garden, *Nature*, 457, 246-247, 2009.



- 877 Rahul, B., K., J. A., and Miaoling, L.: Climate-driven uncertainties in modeling terrestrial gross
878 primary production: a site level to global-scale analysis, *Global Change Biology*, 20, 1394-1411,
879 2014.
- 880 Ranganath, B. K., Pradeep, N., Manjula, V. B., Gowda, B., Rajanna, M. D., Shettigar, D., and
881 RAO, P. P. N.: Detection of diseased rubber plantations using satellite remote sensing, *Journal of*
882 *the Indian Society of Remote Sensing*, 32, 49-58, 2004.
- 883 Rowland, L., da Costa, A. C. L., Galbraith, D. R., Oliveira, R. S., Binks, O. J., Oliveira, A. A. R.,
884 Pullen, A. M., Doughty, C. E., Metcalfe, D. B., Vasconcelos, S. S., Ferreira, L. V., Malhi, Y.,
885 Grace, J., Mencuccini, M., and Meir, P.: Death from drought in tropical forests is triggered by
886 hydraulics not carbon starvation, *Nature*, 528, 119, 2015.
- 887 Sara, P., Günter, H., Anna, S., Christian, K., and Pete, M.: Does carbon storage limit tree
888 growth?, *New Phytologist*, 201, 1096-1100, 2014.
- 889 Senf, C., Pflugmacher, D., van der Linden, S., and Hostert, P.: Mapping Rubber Plantations and
890 Natural Forests in Xishuangbanna (Southwest China) Using Multi-Spectral Phenological Metrics
891 from MODIS Time Series, *Remote Sensing*, 5, 2795, 2013.
- 892 Shi, M., Fisher, J. B., Brzostek, E. R., and Phillips, R. P.: Carbon cost of plant nitrogen
893 acquisition: global carbon cycle impact from an improved plant nitrogen cycle in the Community
894 Land Model, *Global Change Biology*, 22, 1299-1314, 2016.
- 895 Silpi, U., Lacoite, A., Kasempsap, P., Thanysawanyangkura, S., Chantuma, P., Gohet, E.,
896 Musigamart, N., Clément, A., Améglio, T., and Thaler, P.: Carbohydrate reserves as a competing
897 sink: evidence from tapping rubber trees, *Tree Physiology*, 27, 881-889, 2007.
- 898 Sitorus, S. R. P. and Pravitasari, A. E.: Land Degradation and Landslide in Indonesia, *Sumatra*
899 *Journal of Disaster, Geography and Geography Education*; Vol 1 No 2 (2017): *Sumatra Journal*
900 *of Disaster, Geography and Geography Education Volume 1 Number 2 : Disaster*, 2017.
- 901 Tan, Z.-H., Zhang, Y.-P., Song, Q.-H., Liu, W.-J., Deng, X.-B., Tang, J.-W., Deng, Y., Zhou,
902 W.-J., Yang, L.-Y., Yu, G.-R., Sun, X.-M., and Liang, N.-S.: Rubber plantations act as water
903 pumps in tropical China, *Geophysical Research Letters*, 38, n/a-n/a, 2011.
- 904 van Straaten, O., Corre, M. D., Wolf, K., Tchienkoua, M., Cuellar, E., Matthews, R. B., and
905 Veldkamp, E.: Conversion of lowland tropical forests to tree cash crop plantations loses up to
906 one-half of stored soil organic carbon, *Proceedings of the National Academy of Sciences*, 112,
907 9956-9960, 2015.



908 Verhoef, A. and Egea, G.: Modeling plant transpiration under limited soil water: Comparison of
909 different plant and soil hydraulic parameterizations and preliminary implications for their use in
910 land surface models, *Agricultural and Forest Meteorology*, 191, 22-32, 2014.

911 Wauters, J. B., Coudert, S., Grallien, E., Jonard, M., and Ponette, Q.: Carbon stock in rubber tree
912 plantations in Western Ghana and Mato Grosso (Brazil), 2008.

913 White, M. A., Thornton, P. E., Running, S. W., and Nemani, R. R.: Parameterization and
914 sensitivity analysis of the BIOME-BCG terrestrial ecosystem model: net primary production
915 controls, *Earth Interactions*, 4, 1-85, 2000.

916 Wu, J., Albert, L. P., Lopes, A. P., Restrepo-Coupe, N., Hayek, M., Wiedemann, K. T., Guan,
917 K., Stark, S. C., Christoffersen, B., Prohaska, N., Tavares, J. V., Marostica, S., Kobayashi, H.,
918 Ferreira, M. L., Campos, K. S., da Silva, R., Brando, P. M., Dye, D. G., Huxman, T. E., Huete,
919 A. R., Nelson, B. W., and Saleska, S. R.: Leaf development and demography explain
920 photosynthetic seasonality in Amazon evergreen forests, *Science*, 351, 972-976, 2016.

921 Wycherley, P. R.: CHAPTER 3 - The Genus *Hevea* - Botanical Aspects. In: *Developments in*
922 *Crop Science*, Sethuraj, M. R. and Mathew, N. M. (Eds.), Elsevier, 1992.

923 Xu, X., Medvigy, D., Powers, J. S., Becknell, J. M., and Guan, K.: Diversity in plant hydraulic
924 traits explains seasonal and inter-annual variations of vegetation dynamics in seasonally dry
925 tropical forests, *New Phytologist*, 212, 80-95, 2016.

926 Yang, X., Blagodatsky, S., Lippe, M., Liu, F., Hammond, J., Xu, J., and Cadisch, G.: Land-use
927 change impact on time-averaged carbon balances: Rubber expansion and reforestation in a
928 biosphere reserve, South-West China, 2016.

929 Ziegler, A. D., Fox, J. M., and Xu, J.: The Rubber Juggernaut, *Science*, 324, 1024-1025, 2009.

930 Ziegler, A. D., Phelps, J., Yuen, J. Q., Webb, E. L., Lawrence, D., Fox, J. M., Bruun, T. B.,
931 Leisz, S. J., Ryan, C. M., Dressler, W., Mertz, O., Pascual, U., Padoch, C., and Koh, L. P.:
932 Carbon outcomes of major land-cover transitions in SE Asia: great uncertainties and REDD+
933 policy implications, *Global Change Biology*, 18, 3087-3099, 2012.

934

935

936

937

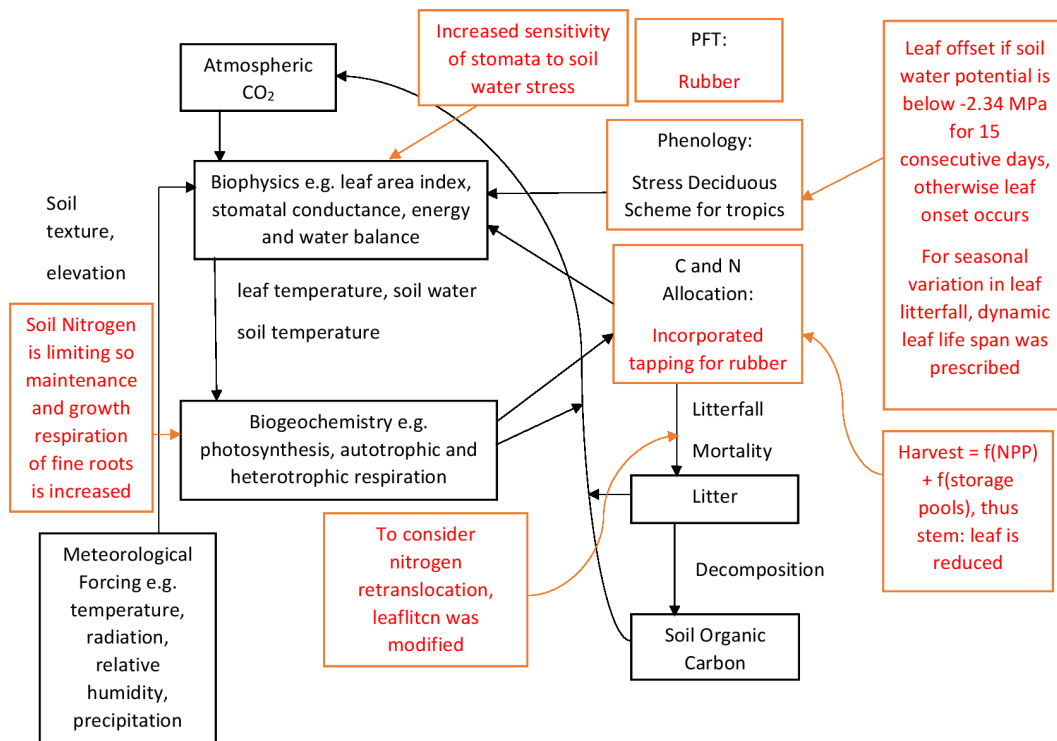
938



941 **Figures**

942 **Figure 1** Illustration of the original and modified structure and functions of CLM4.5 for
 943 incorporating the rubber plant functional type (PFT). The original functions in CLM4.5 are
 944 represented in black while the new rubber PFT in CLM4.5 are represented in red, which includes
 945 changes to phenology, allocation of carbon and nitrogen, and harvest algorithm.

946



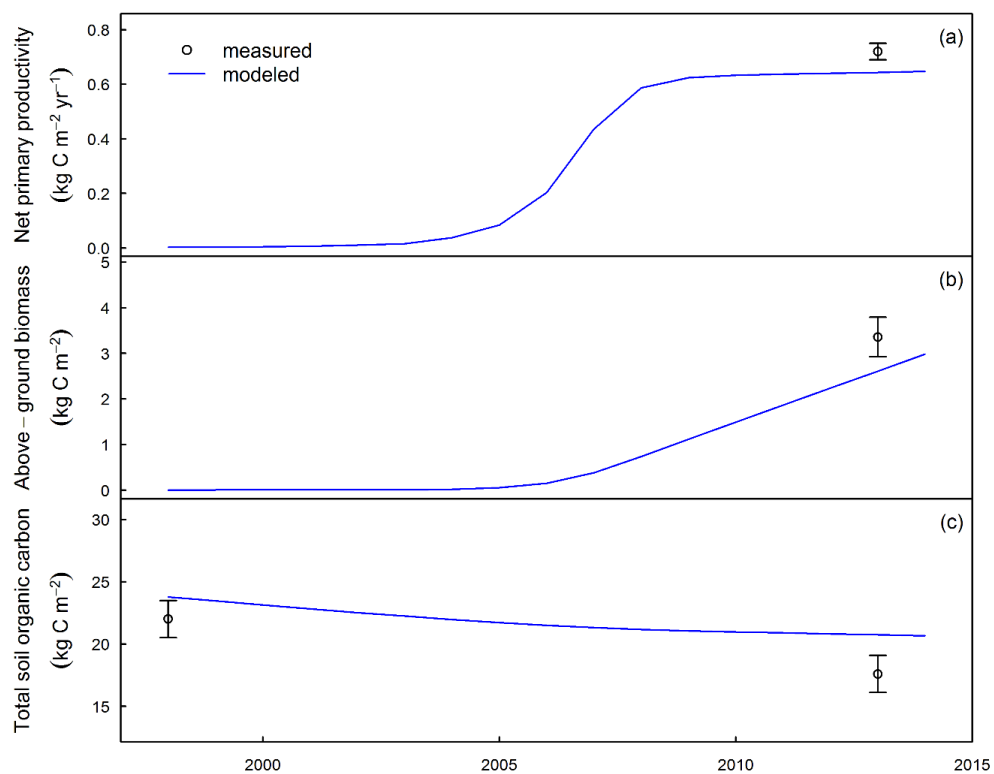
947

948

949



950 **Figure 2** Temporal trends of annual net primary productivity (NPP; $\text{kg C m}^{-2} \text{ yr}^{-1}$) annual above
 951 ground biomass (AGB; kg m^{-2}), and total soil organic carbon content up to 3 m (TSOC; kg m^{-2})
 952 of rubber, simulated by CLM-rubber following clear-cut in 2001 in the Harapan landscape.
 953 Measured NPP, AGB and TSOC (lines are standard errors, $n = 4$ plots) are indicated for 2014.



954

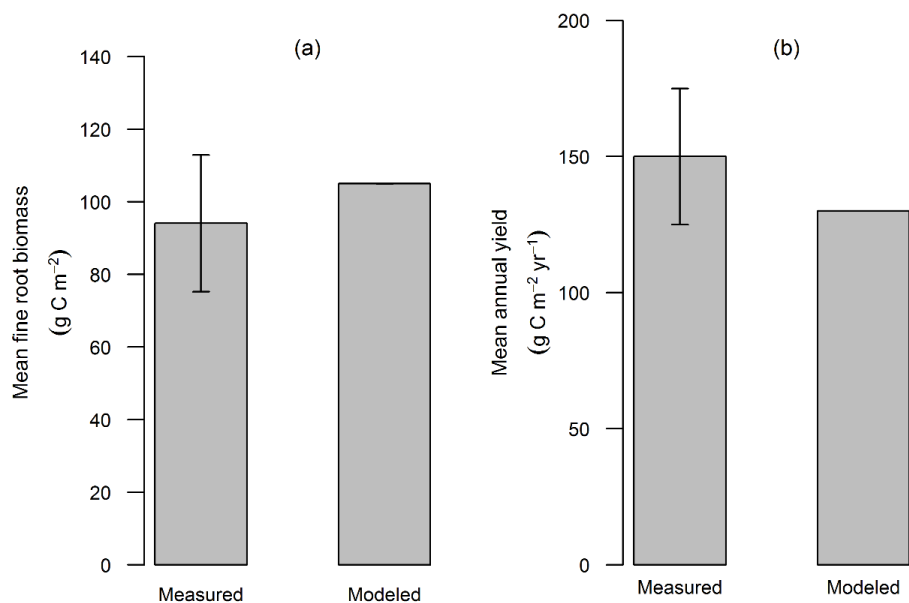
955

956

957



958 **Figure 3** Measured (lines are standard error, $n = 4$ plots) and CLM-simulated fine root biomass
959 (a) and annual latex yield (b) of rubber plantation in 2013 in the Harapan landscape.

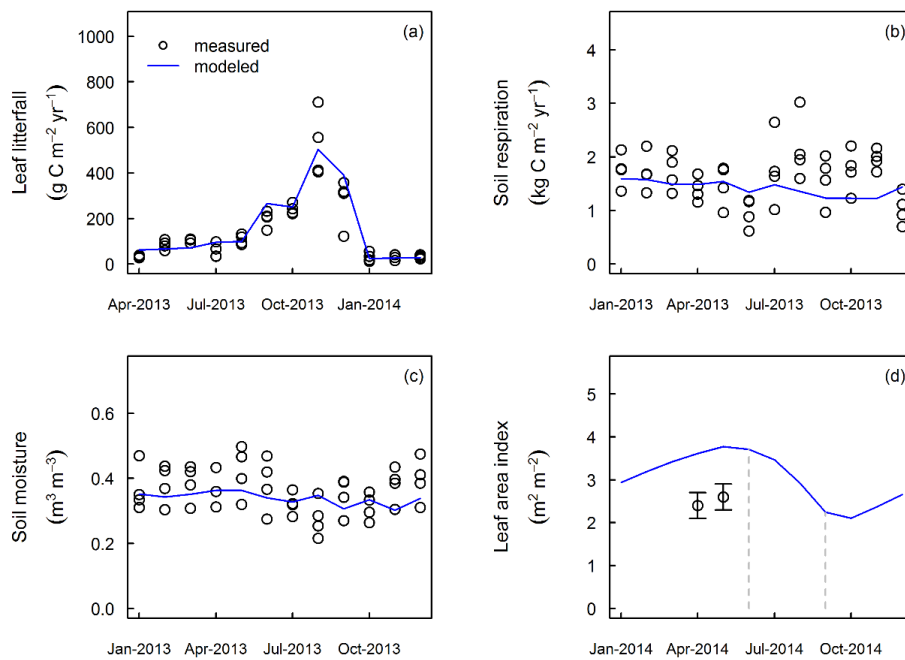


960

961



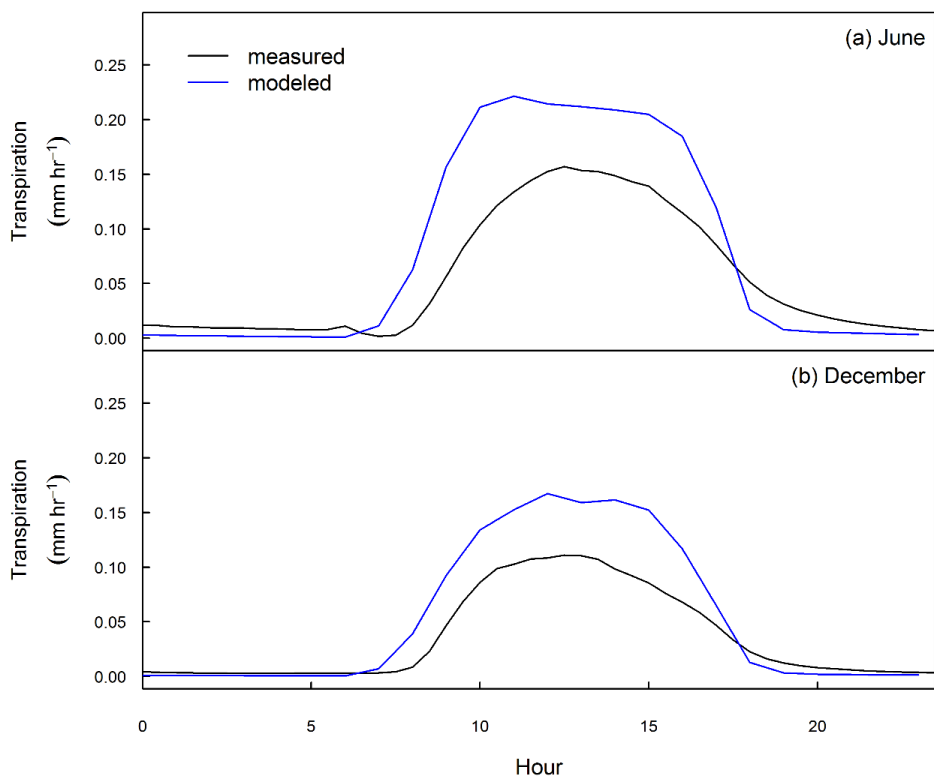
962 **Figure 4** Monthly trends of leaf litter fall ((a); $\text{g C m}^{-2} \text{ yr}^{-1}$),
963 soil respiration ((b); $\text{kg C m}^{-2} \text{ yr}^{-1}$),
964 soil moisture up to 5 cm ((c); $\text{m}^3 \text{ m}^{-3}$) and leaf area index ((d); $\text{m}^2 \text{ m}^{-2}$) of rubber plants simulated
965 by CLM-rubber (blue line) and observed values (open circles) during the mature phase of growth
966 of rubber. The leaf area index (LAI) was measured in 2018. In April, LAI was measured in only
967 one plot whereas in May, LAI was measured across all four plots. The vertical line in April is the
968 standard error across the first plot while the vertical line in May is the standard error across all
four plots.



969
970
971
972
973



974 **Figure 5** Measured and modeled diel transpiration (mm hr^{-1}) of rubber averaged over June (dry
975 month) and December (wet month) in the Harapan landscape in 2013.



976

977

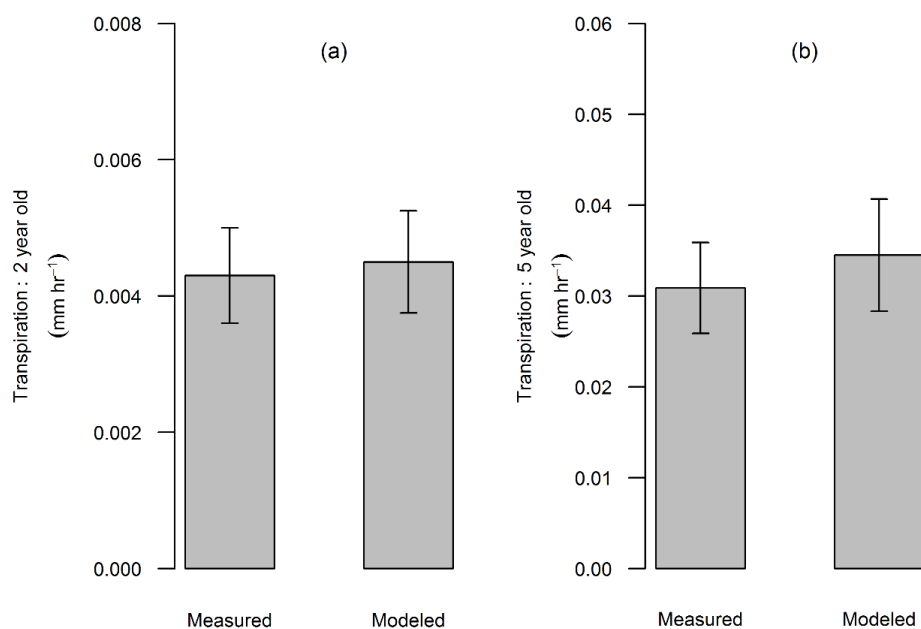
978

979

980



981 **Figure 6** Measured and CLM-simulated transpiration of (a) a 2-year old rubber over December,
982 2013 and (b) a 5-year old rubber over January, 2014 in the Harapan landscape. The bars and the
983 lines are means and standard errors, respectively, over half-hourly data of each month.



984

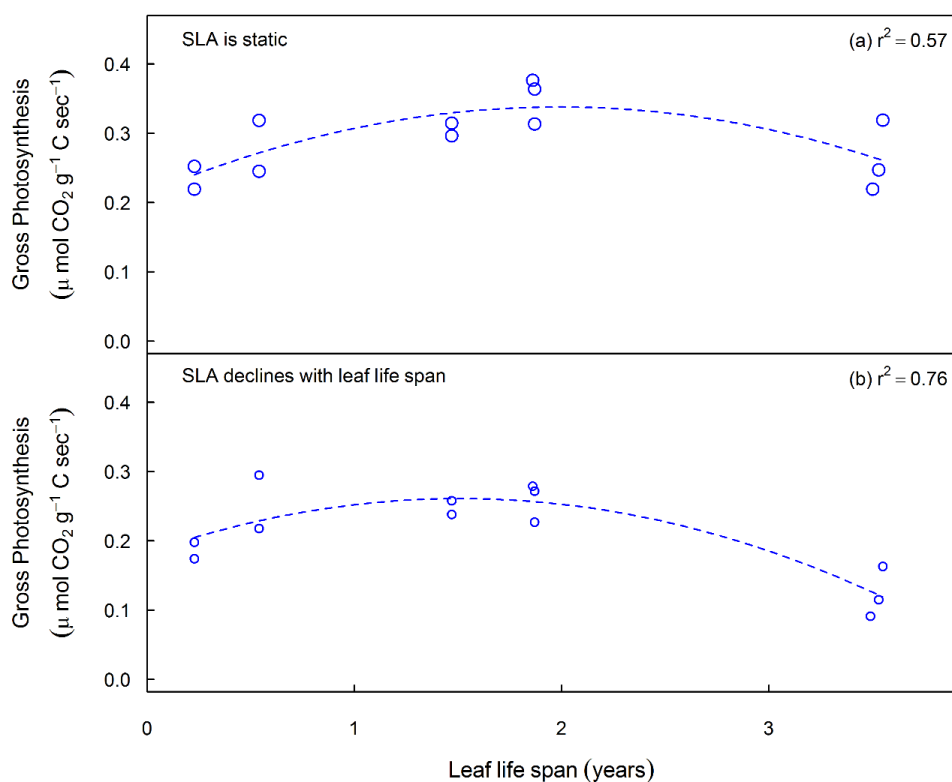
985

986

987



988 **Figure 7** Effect of fixed specific leaf area (SLA) (a) versus dynamic SLA (b) on the CLM-
 989 simulated photosynthesis of rubber leaves, expressed on leaf mass basis, as a function of leaf life
 990 span. Each data point corresponds to the monthly value, which is an average of the peak
 991 photosynthesis between 10 am and 2 pm. The data points corresponding to the lowest leaf life
 992 span belong to the dry season while those at mean leaf life span correspond to the period before
 993 the leaf fall. The data points corresponding to the highest leaf life span correspond to the period
 994 after the leaf fall. The blue dashed line is the best fit with the goodness of fit indicated by the r^2
 995 value.



996

997

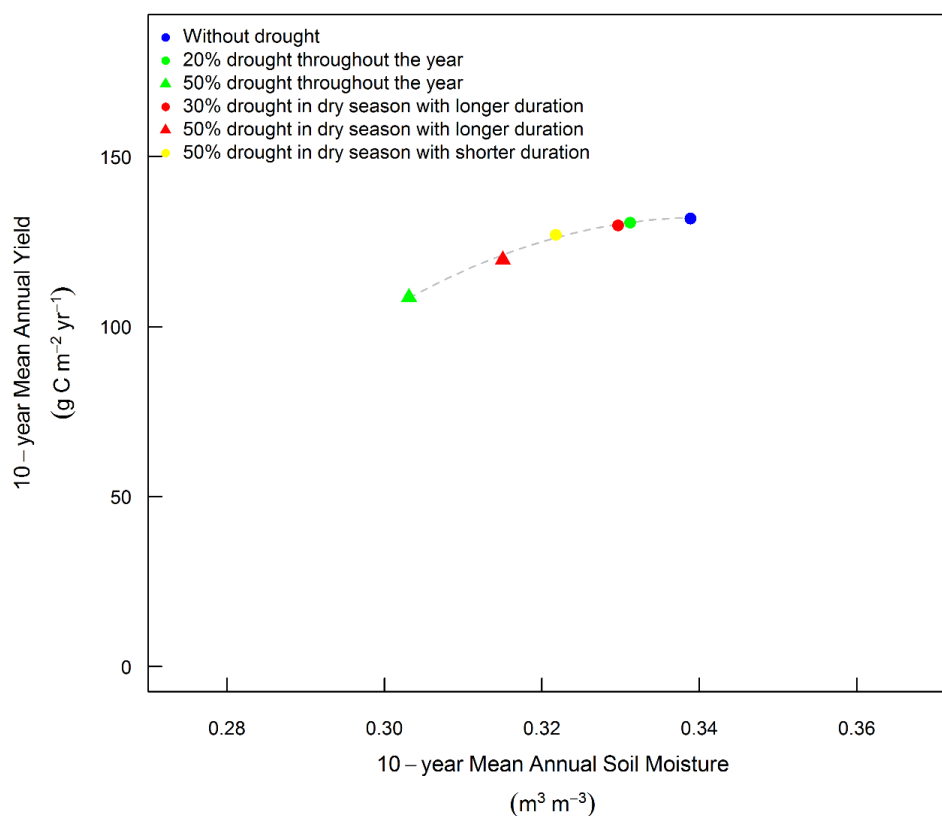
998

999



1000 **Figure 8** Relationship of modeled mean annual latex yield and mean annual soil moisture for a
 1001 rubber plantation over a 10-year period of simulated scenarios. The without drought simulation
 1002 used the default climate conditions while there were five simulations that considered different
 1003 types of drought; two simulations assumed drought to occur throughout the year and so these
 1004 simulations had 20%, 50% lower precipitation than the default precipitation; the other two
 1005 simulations assumed drought to occur with the extended dry season and so precipitation from
 1006 April to October was reduced by 30%, 50%, in these simulations; and the final simulation
 1007 considered shorter dry season but with intense drought so in this simulation precipitation from 8th
 1008 May to 12th September was reduced by 50%.

1009



1010

1011



1012 **Tables**

1013 **Table 1** Summary of net ecosystem exchange (NEE = net CO₂ uptake), latent (LE) and sensible
1014 (H) heat flux densities, and evapotranspiration (ET) estimates for rubber plantations across
1015 Southeast Asia. The italicized values are estimates derived from the CLM-rubber model.
1016 Negative values indicate a flux toward the land surface (= sink) while positive values indicate a
1017 flux toward the atmosphere (= source). R_{net} is net radiation.

1018

Location	Mean NEE of the wettest month (kg C m ⁻² yr ⁻¹)	Mean NEE of the driest month (kg C m ⁻² yr ⁻¹)	Mean Annual Rainfall (mm yr ⁻¹)	Mean Annual R _{net} (W m ⁻²)	Mean Annual ET (mm yr ⁻¹)	Mean Annual Latent Heat (W m ⁻²)	Mean Annual Sensible Heat (W m ⁻²)
Xiushuangbanna, China	NA	NA	1504	123.3	1125	87.4	NA
CRRI, Cambodia	NA	NA	1439	151	1459	112.5	NA
Som Sanuk, Thailand	-2.35	0.68	2145	129.5	1211	93.5	26.9
This study - Jambi, Indonesia	-0.25	0.09	2849	139.4	964	76.4	62.9

1019

1020

1021 **Table 2** Comparison of water fluxes from CLM-rubber with a soil water model (Kurniawan et
1022 al., 2018) that is parameterized with the site-specific characteristics of the rubber plantations in
1023 the Harapan landscape.

1024

	CLM-rubber	Soil Water Model
Transpiration (mm yr ⁻¹)	625	594
Evapotranspiration (mm yr ⁻¹)	964	1077
(Runoff + drainage)/Precipitation (unitless)	0.66	0.68

1025

1026

1027 **Table 3** Comparison among above ground biomass (AGB) of rubber plantations in the tropics
1028 with similar age.

1029

	AGB (kg C m ⁻²)	Source
South-West China	3.92 ± 0.82	Yang et al. (2016)
Western Ghana, Africa	5.72 ± 0.96	Wauters et al. (2008)
Mato Grosso, Brazil	3.12 ± 0.72	Wauters et al. (2008)
Harapan Indonesia	3.36 ± 0.43	Kotowska et al. (2015)
CLM-rubber model for Harapan, Indonesia	2.98	This study

1030